

## Feedbacks between climate and boreal forests during the Holocene epoch

Jonathan A. Foley, John E. Kutzbach,  
Michael T. Coe & Samuel Levis

Institute for Environmental Studies, and Department of Atmospheric and Oceanic Sciences, University of Wisconsin-Madison, 1225 West Dayton Street, Madison, Wisconsin 53706, USA

PREVIOUS studies<sup>1-5</sup> have demonstrated that the predictions of global climate models are highly sensitive to large changes in vegetation cover, such as the complete removal of tropical or boreal forests. Although these studies have illustrated the potential effects of massive deforestation on the climate system, vegetation changes of this scale are very unlikely to occur. Investigating past environments may better illustrate the possible interactions between climate and vegetation cover. For example, palaeobotanical evidence indicates that 6,000 years ago boreal forests extended north of the modern treeline<sup>6</sup>, apparently in response to high-latitude warming resulting from variations in the Earth's orbit<sup>7,8</sup>. The expanded boreal forests, which took the place of tundra, must also have affected climate by significantly reducing the surface albedo<sup>5</sup>. Here we use a global climate model to examine the relative effects of orbitally-induced insolation variations and of the northward extension of boreal forests on the mid-Holocene climate. Orbital variations alone warm the high latitudes by 2 °C or more in summer, autumn and winter. The subsequent northward extension of boreal forests gives rise to an additional warming of approximately 4 °C in spring and about 1 °C in the other seasons. This suggests that large positive feedbacks between climate and boreal forests may have taken place in the recent geological past.

We perform three climate simulations with the GENESIS global climate model (GCM) version 1.02 (refs. 9, 10): Control (control climate simulation), Exp-A (climate simulation with changes in the Earth's orbit) and Exp-B (climate simulation with changes in the Earth's orbit and expanded boreal forests). In all of these simulations atmospheric CO<sub>2</sub> concentrations are held constant. We examine the effects of two forcing mechanisms on the global climate: orbital forcing (Exp-A minus Control) and the subsequent vegetation forcing (Exp-B minus Exp-A).

In Exp-A, we change the Earth's orbital parameters from the modern values to represent conditions 6 kyr ago; eccentricity from 0.0167 to 0.0187, axial tilt from 23.4° to 24.1° and date of perihelion from early January to mid-September<sup>7,8</sup>. The change in the date of perihelion increases the amplitude of the seasonal cycle of Northern Hemisphere insolation by ~5%, leading to enhanced heating in summer and enhanced cooling in winter. The increased axial tilt further enhances high-latitude summer insolation. In the high northern latitudes, increased summer insolation leads to warmer ocean temperatures and delays the formation of sea ice, resulting in warmer winter conditions and hence year-round warming<sup>11</sup>.

Palaeobotanical data indicate that a northward expansion of boreal forests occurred during the middle Holocene<sup>12-19</sup>. This expansion must have resulted, in part, from the orbitally-induced high-latitude warming<sup>14</sup>. In Exp-B, we extend the northern limit of boreal forests based on two criteria: (1) palaeobotanical evidence, which is sparse in many regions, and (2) GCM sensitivity considerations which require that changes in boundary conditions cover several contiguous model grid-cells (Fig. 1). Because of the coarse spatial resolution of the GCM (~4.5° latitude by 7.5° longitude), there are differences between the imposed boreal forest expansion and the palaeobotanical data. For example, in portions of North America, the observed expansion was less extensive than that imposed in our simulations; but in Asia, there is better agreement. In the future it will be possible to repeat these simulations with higher-resolution GCMs and more complete palaeovegetation datasets.

Both orbital forcing and vegetation forcing operate mainly by affecting the amount of solar radiation absorbed by the surface. In response to orbital forcing, annual absorbed solar radiation in the high northern latitudes (defined here as 60–90° N) increases by ~4 W m<sup>-2</sup> (Table 1). On the annual average, vegetation forcing lowers the land surface albedo from 0.36 to 0.26 (Table 1), primarily by replacing snow-covered tundra with an evergreen forest that protrudes above the snow, resulting in an additional 8 W m<sup>-2</sup> absorbed solar radiation. In these simulations, the changes in high-latitude cloud cover are not statistically significant and do not appreciably feed back on the surface energy balance.

On the annual average, orbital forcing warms the high latitudes by 1.8 °C (Table 1, Fig. 2a). Vegetation forcing produces an additional annual-average warming of 1.6 °C (Table 1, Fig. 2b). The largest temperature increases due to vegetation forcing generally coincide with the areas of expanded forest.

FIG. 1 The prescribed extent of boreal forests used in the GENESIS GCM simulations. GENESIS specifies surface properties on a 2° latitude by 2° longitude grid (solid colours), whereas the atmospheric model operates on a 4.5° latitude by 7.5° longitude grid (lines).

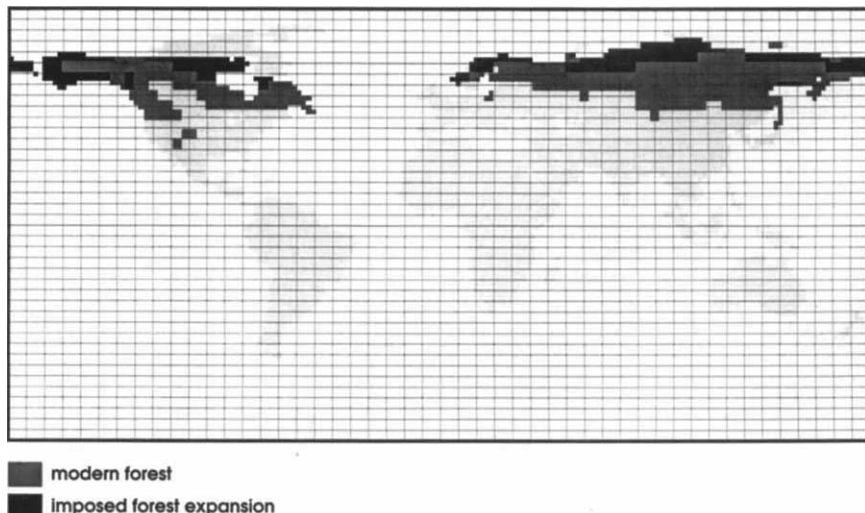


TABLE 1 Simulated climate variables from 60 to 90 °N

	Control	Exp-A	Exp-B
Surface temperature (°C)	-8.4	-6.6	-5.0
Deep soil ice fraction (1.75–4.25 m)	0.31	0.28	0.23
Precipitation (mm d <sup>-1</sup> )	1.73	1.81	1.88
Runoff (mm d <sup>-1</sup> )	0.89	1.00	1.09
Sea ice thickness (cm)	79.0	63.0	56.0
Sea ice fraction	0.52	0.46	0.43
Snow-cover thickness (cm H <sub>2</sub> O)	13.0	11.0	10.0
Snow-cover fraction	0.40	0.34	0.30
Surface albedo, winter	0.434	0.423	0.301
Surface albedo, spring	0.576	0.581	0.414
Surface albedo, summer	0.172	0.166	0.149
Surface albedo, autumn	0.275	0.234	0.182
Surface albedo, annual	0.364	0.356	0.265
Absorbed solar radiation, winter (W m <sup>-2</sup> )	7.3	6.0	6.9
Absorbed solar radiation, spring (W m <sup>-2</sup> )	136.0	135.1	157.1
Absorbed solar radiation, summer (W m <sup>-2</sup> )	253.9	277.4	284.8
Absorbed solar radiation, autumn (W m <sup>-2</sup> )	43.8	49.6	50.9
Absorbed solar radiation, annual (W m <sup>-2</sup> )	111.2	115.3	123.3

Summary of GENESIS climate model simulations for Control (modern), Exp-A (orbital forcing) and Exp-B (orbital forcing + vegetation forcing). All values are annual averages for land only unless otherwise stated. As a general basis of comparison of the sensitivity of this climate model, we note that the GENESIS GCM simulates a global surface temperature warming of 2.1 °C due to doubled atmospheric CO<sub>2</sub>, which is towards the low end of the range in recent climate model experiments<sup>23</sup>.

However, the magnitude and pattern of these changes must be assessed relative to the inherent interannual variability of the GCM<sup>20</sup>. The simulated interannual variability of surface temperature is large across North America from eastern Alaska to Greenland, and small across northern Eurasia. Thus the simulated warming due to vegetation forcing (Fig. 2b) has a higher statistical significance over northern Eurasia than over eastern North America and Greenland. Similarly, the 3 °C warming due to orbital forcing (Fig. 2a) in North America has no higher statistical significance than the 1–2 °C warming elsewhere. Overall, the 1.8 °C annual-average warming due to orbital forcing, and the additional 1.6 °C warming due to vegetation forcing, are both statistically significant at the 95% level.

Although the annual-average temperature changes from both orbital and vegetation forcing are of similar magnitude, the seasonal responses differ significantly (Fig. 3). Under orbital forcing, monthly average temperature changes are >1 °C beginning in June, with a maximum change of ~5 °C in December. Vegetation forcing produces a maximum temperature response of ~4 °C in March and April, and temperature increases of >1 °C occur throughout the year (except in January and October).

Snow and ice cover play an important role in the high-latitude climates. Both orbital forcing and the subsequent vegetation forcing result in similar decreases in snow cover over land and Arctic sea ice (Table 1). Taken together, orbital and vegetation forcing reduce snow and sea-ice volume by nearly 40%. The reduction of the highly reflective snow and ice cover enhances both orbital and vegetation forcing, thus acting as an additional positive feedback mechanism<sup>5</sup>.

The hydrological cycle is strongly affected by both orbital and vegetation forcing. Annual precipitation over high-latitude land increases by ~5% in both simulations (Table 1). The enhanced rate of precipitation results from an increase in the water vapour content of the atmosphere under warmer conditions. Runoff,

which includes surface runoff and subsurface drainage, increases by ~10% in response to both orbital and vegetation forcing. In addition, orbital and vegetation forcing each warm the high-latitude soils and reduce the amount of deep soil ice by ~10%.

Compared to the present day, the climate in the middle Holocene was substantially warmer in the high northern latitudes. Our mid-Holocene climate simulation without vegetation feedbacks (Exp-A) yields a 1.8 °C high-latitude warming, in good agreement with other modelling studies<sup>7,8,11</sup>. However, palaeoclimatic analyses indicate that the annual-average surface temperatures may have been as much as 3 °C warmer than present in northern Eurasia and northern North America in the middle Holocene<sup>21,22</sup>. The large positive feedback due to the northward extension of boreal forests (Exp-B) could help to explain the amount of observed mid-Holocene warmth, which orbital forcing alone does not appear to produce.

The amplification of high-latitude warming shown here may also be relevant to issues of anthropogenic climate change. The

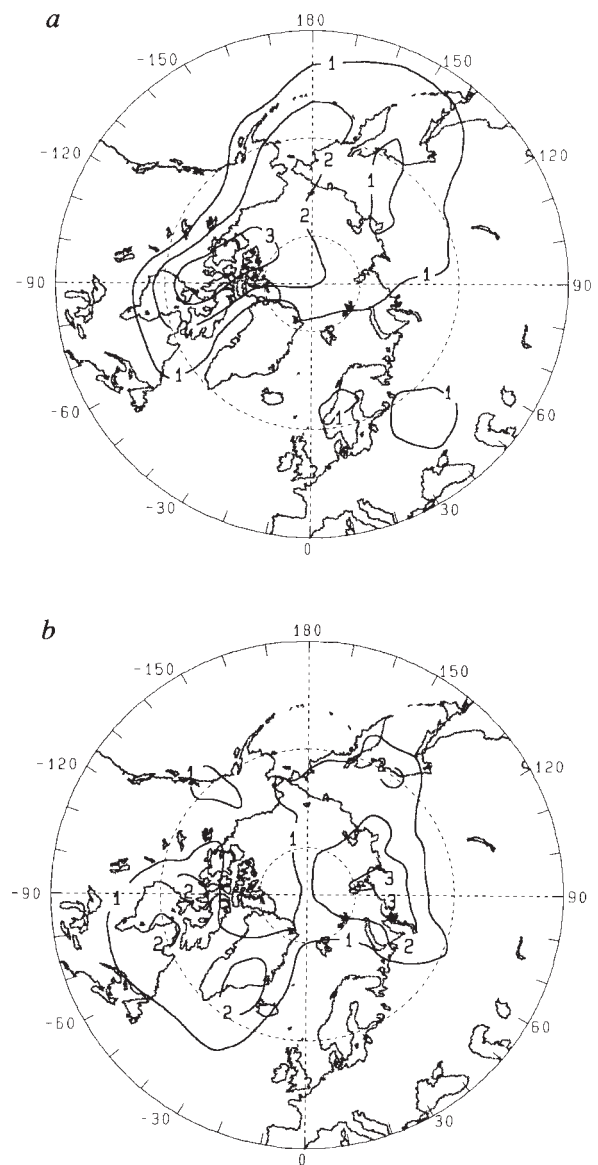


FIG. 2 a, Annual-average surface temperature increases due to mid-Holocene orbital forcing (Exp-A minus Control). Units are in °C; the contour interval is 1 °C. b, Annual-average surface temperature increases due to mid-Holocene vegetation forcing (Exp-B minus Exp-A). Same units and contour interval as a.

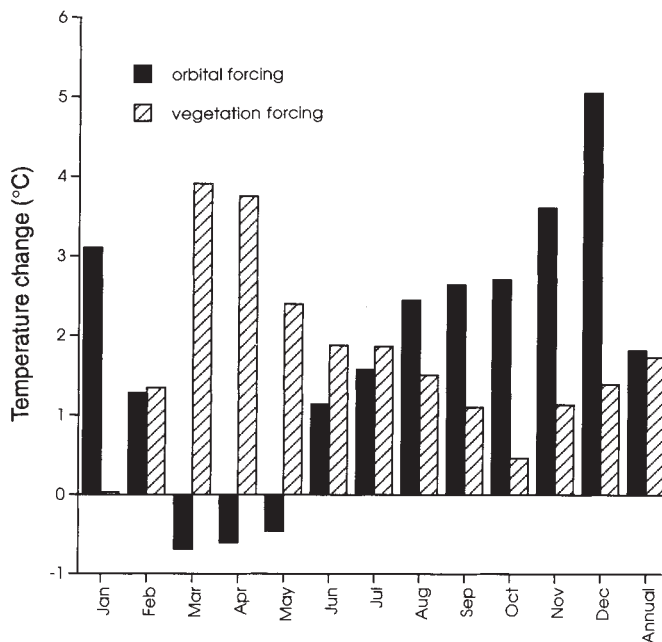


FIG. 3 Changes in zonal-average (over land from 60° to 90° N) monthly surface temperatures due to orbital and vegetation forcing.

estimates of high-latitude warming in response to greenhouse gas emissions<sup>23</sup> may need to be re-evaluated for the effects of possible vegetation feedbacks in light of these results. Further investigations of the interactions between climate and vegetation should be performed with fully coupled models of the climate system (including improved cloud, sea-ice and ocean processes) and the terrestrial biosphere. In addition, improvements in model resolution would depict the shifts in palaeovegetation more accurately than was possible here. □

## A cellular model of braided rivers

A. Brad Murray & Chris Paola

Department of Geology and Geophysics, University of Minnesota, Minneapolis, Minnesota 55455, USA

A BROAD sheet of water flowing over non-cohesive sediment typically breaks up into a network of interconnected channels called a braided stream (Fig. 1). The dynamics of such networks are complex; channels migrate laterally, split, rejoin and develop bars, with the flow shifting unpredictably from one part of the network to another. Many processes are known to operate in a braided river<sup>1-3</sup>, but it is unclear which of these are essential to explain the observed dynamics. We describe here a simple, deterministic numerical model of water flow over a cohesionless bed that captures the main spatial and temporal features of real braided rivers. The patterns arise from local scour and deposition caused by a nonlinear dependence of bedload sediment flux on water discharge. Although the morphology of the resulting network depends in detail on the sediment-transport rule used in the model, our results suggest that the only factors essential for braiding are bedload sediment transport and laterally unconstrained free-surface flow.

Recently, a number of workers have used cellular computer models to study naturally occurring spatial patterns<sup>4-9</sup>. In these models the cells of a lattice interact according to rules based on abstractions of the physics governing a system. Here we present a cellular model of stream braiding (see Box 1). The initial condition for the model is a uniform slope with white-noise elevation perturbations; the latter have an amplitude of the order of the mean downhill elevation difference between adjacent rows of cells. We include high side walls to contain the flow. An iteration begins when water is introduced into some of the cells at the upstream end of the lattice, and begins moving downstream cell-by-cell, carrying sediment. When the water reaches the downstream end of the lattice, the iteration ends, and the elevation

Received 16 March; accepted 28 July 1994.

- Dickinson, R. E. & Henderson-Sellers, A. Q. *Jl R. met. Soc.* **114**, 439-462 (1988).
- Shukla, J., Nobre, C. & Sellers, P. J. *Science* **247**, 1322-1325 (1990).
- Henderson-Sellers, A. et al. *J. geophys. Res.* **98**, 7289-7315 (1993).
- Lean, J. & Rowntree, P. R. Q. *Jl R. met. Soc.* **119**, 509-530 (1993).
- Bonan, G. B., Pollard, D. & Thompson, S. L. *Nature* **359**, 716-718 (1992).
- Ritchie, J.C. *Postglacial Vegetation of Canada* (Cambridge Univ. Press, 1987).
- COHMAP Members *Science* **241**, 1043-1052 (1988).
- Wright, H. E. Jr, et al. (eds) *Global Climates since the Last Glacial Maximum* (Univ. Minnesota Press, Minneapolis, 1993).
- Thompson, S. L. & Pollard, D. *J. Clim.* (in the press).
- Pollard, D. & Thompson, S. L. *Glob planet. Change* (in the press).
- Mitchell, J. F. B., Grahame, N. S. & Needham, K. H. *J. geophys. Res.* **93**, 8283-8303 (1988).
- Bryson, R. A., Irving, W. N. & Larsen, J. A. *Science* **147**, 46-48 (1965).
- Sorenson, C. J., Knox, J. C., Larsen, J. A. & Bryson, R. A. *Quat. Res.* **19**, 1-17 (1972).
- Ritchie, J. C., Cwynar, L. C. & Spear, R. W. *Nature* **305**, 126-128 (1983).
- Khotinsky, N. A. in *Late Quaternary Environments of the Soviet Union* (eds Velichko, A. A., Wright, H. E. Jr & Barnosky, C. W. 179-200 (Univ. Minnesota Press, Minneapolis, 1984).
- Cwynar, L. C. & Spear, R. W. *Ecology* **72**, 202-212 (1991).
- Keenan, T. J. & Cwynar, L. C. *Can. J. Bot.* **70**, 1336-1345 (1992).
- Peterson, G. in *Global Climates Since the Last Glacial Maximum* (eds Wright, H. E. Jr et al.) (Univ. Minnesota Press, Minneapolis, 1994).
- Webb, T., Bartlein, P. J. & Kutzbach, J. E. in *North America and Adjacent Oceans During the Last Glaciation* (eds Ruddiman, W. F. & Wright, H. E. Jr) (Geological Soc. Am., Boulder, Colorado, 1987).
- Kutzbach, J. E. & Guetter, P. J. *J. atmos. Sci.* **43**, 1726-1759 (1986).
- Frenzel, B., Pécsi, M. & Velichko, A. A. (eds) *Atlas of Palaeoclimates and Palaeoenvironments of the Northern Hemisphere: Late Pleistocene-Holocene* (Geographical Res. Inst., Hungarian Acad. Sci. Budapest, 1992).
- Guiot, J., Harrison, S. P. & Prentice, I. C. *Quat. Res.* **40**, 139-149 (1993).
- Houghton, J. T., Jenkins, G. J. & Ephraums, J. J. (eds) *Climate Change: The IPCC Scientific Assessment* (Cambridge Univ. Press, 1990).

ACKNOWLEDGMENTS. We thank S. Thompson and D. Pollard for providing the GENESIS climate model. We also thank P. Behling, R. Gallimore and R. Selin for assistance with the simulations. This manuscript was substantially improved by the comments of J. Mitchell, I. C. Prentice and T. Webb. This research was supported by the US NSF the US DOE and the Climate, People and Environment Program (CPEP) of the University of Wisconsin. The computer simulations were performed at the National Center for Atmospheric Research, which is supported by the US NSF.



FIG. 1 Aerial photograph of part of the braided Aichilik River on the north slope of the Brooks Range in Alaska. Flow is from top to bottom. The slope is ~0.001, the gravel flat is ~0.5 km wide, and the flow depths are of the order of 1 m.